MAINTENANCE-BASED DESIGN OF CONCRETE PARKING STRUCTURES

By

Christopher D. Stoakes

Bachelor of Science in Civil Engineering
University of Iowa, 2003

SUBMITTED TO THE DEPARTMENT OF CIVIL AND ENVIRONEMENTAL ENGIEERING
IN PARTIAL FULFILLMENT OF THE REQUIREMENTS FOR THE DEGREE OF

MASTER OF ENGINEERING IN CIVIL AND ENVIRONMENTAL ENGINEERING
AT THE
MASSACHUSETTS INSTITUTE OF TECHNOLOGY

JUNE 2007

Signature of Author_____

Christopher D. Stoakes
Department of Civil and Environmental Engineering
May 23, 2007

Certified by_____

Daniele Veneziano
Professor of Civil and Environmental Engineering
Thesis Supervisor

Accepted by_____

Daniele Veneziano
Professor of Civil and Environmental Engineering
Chairman, Departmental Committee for Graduate Students

MAINTENANCE-BASED DESIGN OF CONCRETE PARKING STRUCTURES

By

Christopher D. Stoakes

Submitted to the Department of Civil and Environmental Engineering on May 23, 2007 in Partial Fulfillment of the Requirements for the Degree of Master of Engineering in Civil and Environmental Engineering

ABSTRACT

The purpose of this study is to determine what type of preventative maintenance for a concrete parking structure will produce the maximum economic benefit. Existing models for concrete deterioration are analyzed for their accuracy in predicting the service lives of concrete structures and a model appropriate for concrete parking structures is selected. The selected model is modified to account for the unique microclimate that is created within a parking structure and used to create deterioration curves that quantify the fraction of a structure deteriorated at a given time. Several preventative maintenance programs that summarize current practice in the repair of concrete parking structures are created. The programs are analyzed using the selected concrete deterioration model and the method of preventative maintenance that maximizes the net present worth of a concrete parking structure is identified.

Thesis Supervisor: Daniele Veneziano
Title: Professor of Civil and Environmental Engineering

TABLE OF CONTENTS

LIST OF TABLES

LIST OF FIGURES

CHAPTER 1: INTRODUCTION

The repair of deteriorated concrete structures has been a necessary part of infrastructure maintenance for the past few decades. Effective repair has become more crucial during the last five years because escalating material and construction costs for new construction have outpaced concrete repair costs. In addition, service life predictions of new concrete structures are required to justify the expenditure necessary to build them. In light of this fact, current research into the behavior of reinforced concrete has focused on predicting the service life of concrete structures based on the diffusion of chlorides and carbon dioxide into structural elements.

The service life of a reinforced concrete structure is defined as the time required to corrode a certain percentage of the steel reinforcement embedded in the concrete. The corrosion process decreases the cross-sectional area of the reinforcement, which decreases the strength of concrete members, and causes cracking of the concrete around the corroded reinforcement, allowing faster penetration of carbon dioxide and chlorides. Both carbon dioxide and chloride ingress are necessary to initiate the corrosion process.

Carbon dioxide (CO_2) reacts chemically with calcium hydroxide (CaOH) in the concrete microstructure forming calcium carbonate ($CaCO_3$). As the concentration of calcium carbonate increases, the pH of the concrete decreases from its initial alkalinity of 12.5. This reaction continues to occur during the service life of the structure, with carbonation eventually reaching the depth of the steel reinforcement. After the pH of the concrete at this depth drops to 8.8, the passive oxide layer that forms around the reinforcement during curing of the concrete is destroyed by the higher acidity of the concrete. Finally, chlorides that have been diffusing through the concrete at roughly the same rate as the carbonation front are able to initiate corrosion of the steel reinforcement once the passive oxide layer is destroyed (Campbell et al. 1991).

Models of this behavior have been developed for bridges and marine structures where the dominant corrosive species is chloride. Concrete parking structures have been left out of current literature even though their geometry creates a microclimate that is not accurately represented by current models. This microclimate results from the expulsion of carbon dioxide by vehicles traveling through the ramp and increases the carbon dioxide concentration within the structure above normal atmospheric concentrations. The amplification of the carbon dioxide concentration needs to be included in deterioration models if an accurate prediction of the service life of a concrete parking structure is to be obtained.

After modifying existing concrete deterioration models to reflect the microclimate within concrete parking structures, this thesis will answer the following question using the updated model: what preventative maintenance programs are best to economically increase the service life of a concrete parking structure?

The primary reason for solving this problem is extending the service life of concrete parking structures. In the design and evaluation of parking structures, maintenance is typically ignored and actions to extend the life of a structure are delayed until a significant portion of the structure's concrete must be removed and replaced. However, if a maintenance program based on the unique environment of a parking structure is defined before the structure is put into service, future maintenance expenditures can be predicted years in advance and included in maintenance budgets. Knowing the required maintenance costs before they are incurred should reduce the probability of delaying those repairs, which will lead to a longer service life for the structure.

In addition to extending the service life of concrete parking structures, more accurate predictions of the service life will help owners remove their structures from service before the cost of maintaining them exceeds the cost of replacing them. After a structure has met or exceeded its service life, the amount of concrete that has been repaired may exceed the amount of original concrete remaining in the structure. In this case, it may seem that the structure has the same load carrying capacity that it had in its original state, but the reduction in the amount of reinforcement due to corrosion, and the inconsistencies between repair concrete and original concrete combine to lower the ultimate strength of the structure. A lower ultimate strength equates to a lower level of safety, which means that continuing to repair a structure after it has surpassed its service life is more expensive and more dangerous than building a new structure.

Chapter 2 presents a broad overview of concrete deterioration research by dividing the existing literature into three categories: chemical deterioration, concrete repair technology, and detection methods. Chemical deterioration research is concerned with improving existing concrete deterioration models by identifying parameters that affect the deterioration of concrete and creating numerical models to describe observed behavior. Concrete repair technology studies investigate the behavior of concrete repair materials and develop new procedures for strengthening concrete structures that minimize concrete removal. New methods for detecting spalled concrete are also being created by adapting existing radar and sonar technologies to concrete structures.

Chapter 3 provides details on existing models of concrete deterioration. Current models are based on solutions to Fick's Second Law of Diffusion and vary depending on surface boundary conditions. Models by Liang et al. (2001), Amey et al. (1998), and Weyers (1998) are presented. Each study also presents a methodology for predicting the service life of reinforced concrete structures. The applicability of these models to concrete parking structures is briefly discussed and the simplified model derived by Liang et al. (2001) is chosen for use in this study.

Chapter 4 uses the concrete deterioration model presented by Liang et al. (2001) to derive deterioration curves for concrete parking structures. The deterioration curves plot the fraction of a structure deteriorated versus time for a given carbonation rate coefficient. The curves are developed by describing the variation of the carbonation rate coefficient within a structure as a log-normal distribution. A critical depth of carbonation is chosen and the probability that a given location at a given time has a carbonation depth greater than the critical carbonation depth is found. Chapter 4 also suggests a procedure for determining the microclimate effect on the carbon dioxide concentration within a concrete parking structure.

Chapter 5 uses the deterioration curves derived in Chapter 4 to investigate the economic benefits of preventative maintenance of concrete parking structures. Several methods of repair and prevention are discussed and four lifetime maintenance programs based on these methods are identified for investigation. The deterioration curves are used to find the times at which repairs are required for each of these programs and the costs of repair and maintenance are recorded. The amount of revenue generated by the parking structure for each program is also estimated. The present worth of the parking structure is calculated for each strategy and the results analyzed to see if an optimum strategy exists.

Chapter 6 presents the conclusions from the economic analysis performed in Chapter 5.

CHAPTER 2: REVIEW OF CONCRETE DETERIORATION RESEARCH

Interest in the deterioration of reinforced concrete structures began to increase dramatically in the early- to mid-1970s. Given that the majority of the United States' reinforced concrete structures were constructed following World War II it is logical to conclude the heightened interest was due to observed deterioration; after 20 to 30 years of service we would expect to see the first signs of concrete failure. Research into the deterioration of concrete focused on predicting service life by modeling the diffusion of carbon dioxide and chlorides through concrete and the corrosion of reinforcing steel.

Since the construction cost of new concrete structures has steadily increased over the past few decades, the ability to repair deteriorated portions of existing structures has become increasingly important. Therefore, current reinforced concrete research is focused on developing new repair materials and methods as well as improving existing deterioration models. In addition, surface coating materials that can prevent the ingress of carbon dioxide and/or chlorides have become popular as a means to lengthen the service life of concrete structures. Consequently, researchers have begun to examine the benefits of these materials and their ability to protect concrete.

Finally, efforts have been made to improve on the traditional methods to detect failed concrete. Areas of concrete deterioration, called spalls, are located by dragging a steel chain across the concrete surface and listening for a "hollow" sound. This sound is the result of the reinforcing steel being transformed into iron-oxide by the corrosion process. The iron-oxide has a lower density than reinforcing steel, which causes the reinforcement to expand and induce stresses in the concrete surrounding the reinforcement. The chain-drag method is well suited for locating areas of spalled concrete, but is not precise enough to evaluate the actual quantity of spalled concrete. Researchers have begun employing radar and sonar techniques to speed-up and increase the accuracy of spall detection.

What follows is a brief review of new advances in concrete chemical deterioration, concrete repair, and deterioration detection.

2.1 CHEMICAL DETERIORATION

For the most part, research on concrete deterioration is focused on predicting the service life of concrete structures based on the time it takes for chlorides and carbon dioxide to diffuse through the concrete surface. The first research conducted in this area was by Z. P. Bazant in the late-1970s. Bazant established a bilinear relationship between the degree of deterioration and time. Degree of deterioration is defined as the reduction in load carrying capacity that results from concrete deterioration. An example of Bazant's graph is shown in Figure 1.

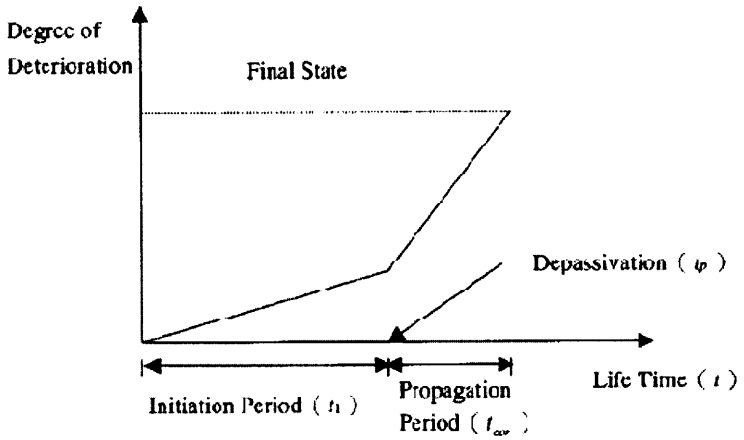

Figure 1

The bilinear form of the graph reflects the different rate of deterioration during the Initiation Period and the Propagation Period. The rate of deterioration during the Initiation Period is much slower because this phase corresponds to the diffusion of carbon dioxide and chlorides through the concrete. Once corrosion starts (Propagation Period), the rate of deterioration is much faster.

By collecting field data and developing empirical formulas, Bazant (1979b) and Guirguis (1987) found that the length of the initiation period is inversely proportional to the Diffusion Coefficient, D_C, of the concrete surface in Fick's Second Law of Diffusion

$$\frac{\partial \varphi}{\partial t} = D_C \frac{\partial^2 \varphi}{\partial t^2} \tag{1}$$

where φ is the substance concentration in mol/m^3 and x is the position in m.

Recent studies have shown more accurate solutions to Fick's Second Law of Diffusion can be determined by solving for the chloride or carbon dioxide concentration as a function of depth and time rather than aiming directly for the time-to-initiation of corrosion. Amey et al. (1998), Weyers (1998), and Liang et al. (2001) have all developed equations of this form. This approach is more accurate because the concentration of carbon dioxide and chloride at the depth of the rebar which initiates corrosion has been determined by previous research. Therefore, knowing the specific concentration needed and the depth it must occur at, the time to initiation can be found by backwards-solving one of the equations.

A more thorough examination of the current concrete deterioration models is presented in Chapter Three.

The studies mentioned above assume a constant source concentration of carbon dioxide or chlorides and do not allow for variations in the diffusion coefficient D_C, also known as diffusivity. Zhang and Gjorv (2005) have shown that the diffusion coefficient of concrete decreases as the source concentration increases. In a numerical model for concrete carbonation, Saetta (2005) incorporated the variability of D_C with temperature and relative humidity. Both approaches make the results more accurate at the expense of complicating the equations.

Puatatsananon and Saouma (2005) researched the coupling between the diffusion of chlorides and the diffusion of carbon dioxide. Since there are a limited number of pores in a concrete sample, the chlorides and carbon dioxide molecules will not diffuse at their maximum rates. Puatatsananon and Saouma were able to model the reduction in diffusivity based on the concentration of carbon dioxide at a given depth of

penetration (carbon dioxide reacts with concrete forming calcium carbonate which decreases its porosity). Thus, considering diffusion of both species decreases the time to initiation of corrosion.

On the other hand, cracks and other variations in the concrete surface tend to accelerate the deterioration of concrete. Lindquist et. al. (2006) and Song et. al. (2005) have shown that cracks create concentration points for chlorides and carbon dioxide. As a result, the corrosion initiation threshold may be exceeded within the first year of service of a particular structure. The problem is exacerbated by higher strength concrete, which has a higher incidence of tensile cracking during the concrete curing period.

Modern concrete admixtures, such as fly ash, silica fume, and blast-furnace slag also contribute to the acceleration of deterioration. Sulapha et al. (2003) showed that concrete mixtures containing any of the above admixtures have lower resistance to carbonation unless special curing procedures are used to insure full hydration of the cement paste. Khunthongkeaw and Tangtermsirikul (2005) have shown a direct correlation between higher fly ash content and lower carbonation resistance.

2.2 CONCRETE REPAIR TECHNOLOGIES

During the early years of concrete repair, the only material used to replace the deteriorated concrete was more concrete. However, it was soon discovered that the long curing period required for concrete was not conducive to quick repair work. Quick repairs are required because the structures that are in need of repair, bridges and parking garages for example, cannot be closed for extended periods of time without a large burden placed on the owner and users of the structure. Therefore, researchers quickly developed repair mortars that cured quickly and achieved high compressive strength just a few days after placement.

Researchers are now focusing on how these materials interact with the existing structure and how well they perform for long periods of time. Consequently, the most investigated aspect of these materials is their ability to bond to the substrate concrete. Minoru et al. (2001) used three-point bending tests on specimens composed of half repair mortar, half substrate concrete to show that the primary load transfer mechanism between the patch material and the substrate concrete is friction. However, these authors also found that the tensile bond between the repair material and the concrete substrate was much weaker at the edges of a repair than in the middle. The result is a patch with a lower strength and durability than the surrounding concrete.

Repair materials with short-duration curing periods are also susceptible to cracking problems. Baluch et al. (2002) showed that typical repair mortars have lower energy of fracture than portland cement concrete, which leads them to develop more cracks than typical concrete and causes them to be more vulnerable to ingress of chlorides and carbon dioxide.

Concrete repair on vertical surfaces, such as the sides and bottom of concrete beams, is even more difficult than repair on horizontal surfaces. It has already been mentioned that the bond strength of repair mortars is suspect (it is not possible to use concrete to repair vertical surfaces since the aggregate is too large) and the higher stress levels in beams cause many of these repairs to fail. To combat this problem, new techniques are being developed that do not require the removal and replacement of concrete from a beam. Branco et al. (2003) investigated the feasibility of bonding steel plates to the sides and bottom of concrete beams using epoxy adhesive to increase their shear and bending capacity. They found that this procedure was effective only for small repair areas. In particular, the strength of these repairs declines rapidly as temperature increases because the epoxy loses its adhesion at temperatures around 100 degrees Fahrenheit.

Wang et al. (2004) have shown that a similar type of repair, using fiber-reinforced plastic (FRP), is feasible for larger repairs. These authors showed that wrapping the sides and bottom of concrete beams with several U-shaped FRPs and then connecting the U-shapes with longitudinal FRPs along the sides of the beam increases the bending capacity of deteriorated concrete beams.

Instead of waiting for concrete to deteriorate and then repair it, one may apply coating products to the surface of concrete structures to prevent diffusion of carbon dioxide and chlorides. There are two types of products that fall into this category: waterproofing membranes, which sit on top of the concrete substrate, and penetrating sealers, which fill the pores in the concrete. The effectiveness of these prevention strategies is currently being investigated. Ibrahim et al. (1999) used accelerated testing on six types of sealers and water proofing membranes to quantify their resistance to chloride and carbon dioxide ingress. Their tests revealed that the only way to prevent carbonation is to use a waterproofing membrane, while chloride diffusion is only slowed by membranes and sealers.

2.3 DETECTION METHODS

As previously mentioned the chain-dragging method is reliable for detecting spalling but is not effective at quantifying the amount of concrete that needs to be removed. Two new technologies being used in place of chain-dragging are Ground Penetrating Radar (GPR) and Impact Echo (IE). The GPR system uses radar technology to look into the concrete structure and find reinforcing steel that exhibits excessive section loss because of corrosion. Like chain-dragging, GPR is excellent for locating spalls but poor at quantifying the repair quantities. Another disadvantage of GPR is the slowness of the detection process.

Impact Echo, a sonar based system, is excellent at finding deteriorations and determining their quantities as well as being quick and easy to perform. However, the IE instrument can only measure deterioration relative to a given threshold value. Gucunski et al. (2005) studied the idea of establishing the threshold value for the IE based on GPR results. Their work showed that it is possible to use GPR for this purpose, but the IE method needs to be recalibrated for different sections of a given bridge deck, depending on the extent of the existing deterioration, i.e. it was not sufficient to make one calibration for the entire bridge. These methods may become more useful in the future, but will not see wide-spread use until they become more reliable and economical.

CHAPTER 3: CURRENT CONCRETE DETERIORATION MODELS

Numerical models of concrete deterioration were first developed in the mid-1970s. These early models were empirical formulas based on observed deterioration of existing structures and attempted to quantify the time it would take for a concrete structure to reach a specified amount of deterioration. Recent research has found that more accurate results may be obtained by modeling the diffusion of molecules through the porous concrete medium. The latter models quantify the concentration of carbon dioxide or chlorides at a certain depth and time instead of solving for the time directly. The time to a critical level of deterioration can be obtained by backwards-solving these equations for a given carbon dioxide or chloride concentration at a specific depth. The rest of this chapter presents the current standards for predicting the service life of concrete structures.

3.1 EVALUATING THE CARBONATION DAMAGE TO CONCRETE BRIDGES USING A GREY FORECASTING MODEL COMBINED WITH A STATISTICAL METHOD (Liang et al. 2001)

The purpose of this study was to improve existing statistical models of concrete deterioration by combining a statistical method with a grey forecasting model. Rather than observing data from a system and approximating that system by a probability distribution, grey forecasting uses original data observations and assumes each stochastic variable is a quantity that varies within a given range. A first-order, linear differential equation is then assumed to describe the rate of change of the observed data. Grey forecasting is beyond the scope of the present study. Therefore, the discussion here focuses on the development of the statistical model. The improved model was used to predict the carbonation depth after 50 years of service for several bridges in Taipei, and the results compared to the carbonation depths predicted from existing models.

The statistical model presented by Liang et al. (2001) is based on Fick's Second Law of Diffusion, Equation (1). These authors solution for the carbon dioxide concentration at depth x and time t is

$$C(x,t) = \left[C_i + \left(C_S e^{kt} - C_i\right) erfc\left(\frac{x}{\sqrt{4D_C t}}\right)\right] e^{-kt} \tag{2}$$

where C_i is the initial CO_2 concentration of the structure, C_S is the CO_2 concentration at the concrete surface, D_C is the concrete diffusivity, and k is a constant. If the CO_2 concentration, $C(X_0, t)=C_0$, is known, Liang et al. (2001) showed that Equation (2) leads to the following expression for the depth of carbonation

$$X_0 = K\sqrt{t} \tag{3}$$

where X_0 is the depth of carbonation and K is the carbonation rate coefficient, a higher K equating to a lower resistance to carbonation. K may be expressed as

$$K = \sqrt{4D_C t} \cdot erfc^{-1}\left(\frac{C_0 e^{kt} - C_i}{C_S e^{kt} - C_i}\right) \tag{4}$$

The authors observe that there is little data available to calibrate K for this model, so they take K as a random variable with normal distribution. Then, X_0 may be expressed as

$$X_0 = (\mu_K + \beta\sigma_K)\sqrt{t} \tag{5}$$

where μ_K and σ_K are the mean and standard deviation of K and β is a random variable with standard normal distribution.

To evaluate μ_K and σ_K, Liang et al. obtained concrete samples from several bridges in Taipei. The carbonation depth was measured from the cores by spraying them with a phenolphaline solution, which changes from a clear to a colored liquid in an acidic environment. The service lives of the bridges were also known. The carbonation rate coefficient was calculated from Equation (3) and the mean and standard deviation for each structure was then determined.

Finally, the depth of carbonation at t=50 years was calculated from the improved statistical model and the resulting carbonation depths compared to existing research. It was assumed that 95% of the structure had reached a specified carbonation depth, which corresponds to β=1.645. The authors concluded that existing statistical models of concrete carbonation overestimate the rate of carbonation, leading to carbonation depth predictions that are greater than carbonation depths observed in real structures. The authors also concluded that the grey forecasting model was able to reduce the difference between observed and predicted carbonation depths. The authors' numerical results are presented in Table 1 below.

Bridge names*	Service life (yrs)	Test points	Statistical method		Proposed method	
			K $\left(mm/(yrs)^{\frac{1}{2}}\right)$	x_0 (mm)	K $\left(mm/(yrs)^{\frac{1}{2}}\right)$	x_0 (mm)
A	49	6	1.824	12.90	1.443	10.20
B	20	20	4.314	30.50	4.233	29.93
C	26	6	1.481	10.47	2.124	15.02
D	18	12	3.015	21.32	3.177	22.46
E	26	8	3.788	26.79	3.595	25.42
F	15	18	3.489	24.67	3.018	21.34
G	24	20	2.116	14.96	1.615	11.42
H	14	10	2.860	20.22	2.373	16.78
I	24	20	3.015	21.32	2.570	18.17

*: A–Huey-tong bridge, B–Beei-men viaduct, C–Way-shuang rivulet bridge, D–Her-pyng west road viaduct, E–Jzyh-chyang bridge, F–Ay-gwo west road viaduct, G-old Hwan-nan viaduct, H–Daw-nan bridge and I–Shi-yuan bridge

Table 1

3.2 TEMPERATURE DEPENDENCE OF COMPRESSIVE STRENGTH OF CONVERSION INHIBITED HIGH ALUMINA CEMENT CONCRETE (Amey et al. 1998)

This study was undertaken to develop a procedure for evaluating concrete mix designs by predicting the service life of a marine structure from the proposed concrete mix. Instead of applying a single deterioration model to an entire structure, the authors divide marine structures into three zones with different deterioration environments. Deterioration models specific to each environment are developed and a procedure for evaluating a concrete mix design is created based on the deterioration models.

The first deterioration zone identified by the authors is the Submerged Zone. Any structural element that is below the water level at high tide is part of this zone. The authors consider the submerged zone to have

a constant surrounding environment, because the chloride content of sea water is relatively constant. This environment can be considered a constant surface boundary condition, which leads to the following solution to Fick's Second Law of Diffusion

$$C(x,t) = C_O\left[1 - \text{erf}\left(\frac{x}{2\sqrt{D_C t}}\right)\right] \tag{6}$$

where C_0 is the surface chloride concentration and D_C is the concrete diffusivity; C_0 and D_C are taken as constants in Equation (6). Given a value X, typically the depth of the steel reinforcement where corrosion initiates, and assuming C_0 and D_C to be known, the service life of structural elements in the submerged zone can be calculated from Equation (6).

The second zone is characterized by an environment that changes with time. In this case the surface chloride concentration must be modeled as a function of time. This zone is called the Splash Zone and is defined as the area directly above the water line where structural elements are regularly moist because of splashing from the waves. In addition, elements in this zone are attacked by chlorides that are suspended in the air directly above the water surface. The surface boundary conditions for this case are defined by

$$C(x,0) = 0 \tag{7}$$

and

$$C(0,t) = \Phi(t) \tag{8}$$

where $\Phi(t)$ is a function of time that describes the buildup of chlorides on the concrete surface. The authors identify two models for $\Phi(t)$: linear and square-root buildup. For linear build-up, $\Phi(t) = kt$ and the solution to Fick's Second Law is Equation (9); for square-root buildup, $\Phi(t) = k\sqrt{t}$ results in Equation (10).

$$C(x,t) = kt\left\{\left(1 + \frac{x^2}{2D_C t}\right) erfc\left(\frac{x}{2\sqrt{D_C t}}\right) - \left(\frac{x}{\sqrt{\pi D_C t}}\right) e^{-x/4D_C t}\right\} \tag{9}$$

$$C(x,t) = k\sqrt{t}\left\{e^{-x^2/4D_C t} - \left[\frac{x\sqrt{\pi}}{2\sqrt{D_C t}} erfc\left(\frac{x}{2\sqrt{D_C t}}\right)\right]\right\} \tag{10}$$

The service life of splash zone components can be predicted with Equations (9) and (10), but the rate of chloride buildup must be measured or assumed so the proper deterioration equation can be used.

The final zone defined by the authors is the Superstructure Zone. Structural elements that are far enough above the waterline to not be affected by air borne chlorides are placed in this category. The deterioration equations used to predict the service life in the splash zone are also used to predict the service life of superstructure components. However, several modifications must be made to the equations.

Surface Chloride Buildup – The surface chloride buildup on superstructure components is not as regular as the buildup in the splash zone. Specifically, the surface chlorides are primarily the result of deicing salts applied to the superstructure during winter months in cold climates. This means the rate of chloride buildup on the superstructure will vary throughout the year and service life predictions must account for seasonal changes in the rate of chloride increase.

Chloride Diffusivity Variation with Temperature – This modification to the deterioration equations is primarily a concern in climates with large differences between high and low temperatures throughout the year. Typically, the chloride diffusivity for a structure is measured at a pre-determined temperature and then converted to a representative diffusivity by the Nernst-Einstein Equation

$$D_2 = D_1 \left(\frac{T_2}{T_1}\right) e^{\left[q\left(\frac{1}{T_1}-\frac{1}{T_2}\right)\right]} \tag{11}$$

where D_1 is the diffusivity measured at temperature T_1, D_2 is the diffusivity at the desired temperature T_2, and q is a constant determined experimentally. The desired temperature is taken as the average daily temperature for a given location.

Construction Variability – In the preceding service life predictions, the depth of the steel reinforcement, X, was assumed constant to simplify service life calculations of structural elements. However, X is not constant and should be modeled as a random variable with a normal distribution

$$X = d - \alpha\sigma \tag{12}$$

where X is the actual depth of reinforcement, d is the design depth of reinforcement, α is a factor that allows X to represent the effective depth corresponding to a given percentage of steel reinforcement that is at a given depth or less from the surface, and σ is the standard deviation. The inclusion of this variability is most appropriate for superstructure components because they are the most likely to be cast-in-place. However, the authors observe that very little data quantifying the standard deviation for this distribution is available; they suggest a value of 8-mm for the standard deviation.

Equations (6), (9), and (10) were developed to find T_i the time-to-initiation of corrosion. The service life of a structure T_{sl} is slightly larger than this value because significant strength loss does not occur until the corrosion has spread to a significant portion of the structure. The authors state that exact models of this behavior are still being developed, but believe a qualitative determination of the time-to-significant damage, T_{SD}, should be included in the service life prediction of concrete structures. The authors' methodology for determining the service life of structural components is summarized in Table 2.

	Submerged	Splash	Superstructure
1	Measure D_C	Measure D_C	Measure D_C
2	Obtain $Temp_{water}$	Obtain $Temp_{season}$	Obtain $Temp_{season}$
3	Calculate $D_C(T)$	Calculate $D_C(T)$	Calculate $D_C(T)$
4	Use C_O = water value	Use C_O = water value	Use $\Phi(max)$ = experience
5	No environment buildup	No environment buildup	Obtain $\Phi(t)$
6	Choose failure criteria	Choose failure criteria	Choose failure criteria
7	Choose σ	Choose σ	Choose σ
8	Choose d	Choose d	Choose d
9	Find X	Find X	Find X
10	Find T_i	Find T_i	Find T_i
11	$T_{sd} = f(quality, T)$	$T_{sd} = f(quality, T)$	$T_{sd} = f(quality, T)$
12	Calculate T_{sl}	Calculate T_{sl}	Calculate T_{sl}

Table 2

3.3 SERVICE LIFE MODEL FOR CONCRETE STRUCTURES IN CHLORIDE LADEN ENVIRONMENTS (Weyers 1998)

The concrete deterioration model suggested in this study is a solution to Fick's Second Law of Diffusion and is similar to the models presented earlier in this chapter. This solution has the form

$$C(x,t) = S\sqrt{t}\left[1 - erf\left(\frac{x}{2\sqrt{D_C t}}\right)\right] \tag{13}$$

where C(x,t) is the CO_2 concentration at depth x and time t, S is the chloride ion concentration, and D_C is the concrete diffusivity. Equation (10) gives the carbon dioxide concentration at depth x and time t and is similar to Equation (6). The author goes on to show that S becomes constant at a depth of 10-mm below the concrete surface. Above this depth, the chloride ion concentration varies based on a number of environmental factors, including moisture and temperature.

In addition to deriving a time-to-initiation model, the author presents a model to calculate the time from corrosion initiation to the end of a structure's service life. Because this study focused on bridge structures, the author defines the end of service life based on the deterioration of the riding quality of the concrete bridge deck, typically judged by a reduced traffic speed. The time at which this occurs can be approximated by the time between initiation of corrosion and cracking of the concrete substrate. The author's model for predicting the time-to-cracking t_{CR} is

$$t_{cr} = \frac{W_{crit}^2}{2k_p} \tag{14}$$

where $k_P = 0.098(1/\alpha)\pi D i_{CORR}$, α=0.57, D is the diameter of reinforcing steel, and i_{CORR} is the annual mean corrosion current density. W_{CRIT} is the critical weight of corrosion products and is given by

$$W_{CRIT} = \rho_{RUST}\left[\pi(d_S + d_O)D + \frac{W_{ST}}{\rho_{ST}}\right] \tag{15}$$

where ρ_{RUST} is the density of corrosion products, d_S is the thickness of corrosion products needed to generate tensile stresses, d_O is the thickness of pore band around the steel/concrete interface, W_{ST} is the weight of steel and ρ_{ST} is the density of steel. The author notes that the values of d_S and d_O may be found in the literature.

In general, Equations (14) and (15) describe the process of the corrosion products exerting pressure on the concrete substrate because they have a lower density than reinforcing steel, i.e. as reinforcing steel corrodes it expands. Eventually, a critical mass of corrosion products is reached and the stresses induced by the corrosion products exceed the tensile stress of the concrete. Based on this model, the typical time to cracking is found to be one to three years after corrosion initiates. Because the time-to-cracking is much smaller than the time-to-initiation of corrosion, the author concludes that it is not necessary to account for time-to-cracking in most service life models for reinforced concrete structures.

3.4 SUMMARY

Concrete deterioration is modeled by solutions to Fick's Second Law of Diffusion. The solutions change depending on the variation of the surface boundary conditions with time. The service life of concrete structures can be predicted from these models if the carbon dioxide concentration C_0 at a depth X_0 and the diffusivity of the concrete are known. Because extreme accuracy is not required from service life predictions during design of a parking structure, plus/minus 5-percent is expected, the models discussed can be simplified to Equation (3). Equation (3) provides acceptable service life predictions for parking structures and will be used for this study.

CHAPTER 4: CARBONATION MODEL FOR CONCRETE PARKING STRUCTURES

The previous section presented formulas that may be used to predict the service life of a reinforced concrete structure. However, it is difficult to quantify the parameters for these functions because these parameters cannot be predicted before a structure is constructed. For example, the diffusivity of concrete is a function of a number of variables, but is most directly correlated to the water-cement ratio of the concrete mixture. Design specifications require this ratio to be within a certain range to insure the concrete gains adequate strength, but it is extremely difficult to control the diffusivity for a large structure that is formed by placing concrete on many different days throughout the year. As a result, the diffusivity of the concrete varies from point-to-point within large structures.

4.1 CARBONATION MODEL

To begin making predictions about the service life of parking structures, a simplified deterioration model needs to be developed that incorporates current understanding of concrete carbonation. The starting point is the simplified carbonation model presented by Liang et al. (2001). These authors found that the depth of carbonation X_0 (mm) may be expressed as

$$X_0 = K\sqrt{t} \tag{16}$$

where t is time in years and K is the carbonation rate coefficient (mm/yr$^{1/2}$). In this model, K is typically taken as a random variable with a normal distribution. Liang et al. (2001) took concrete samples from several bridges in Taipei and measured the carbonation depth of the samples. The service lives of the bridges were also known. The results of these experiments are presented in the following table.

Bridge Name*	Date of Completed Construction (A.D.)	Service life (yrs)	Test points	Carbonation depth x_0 (mm)			Coefficient of carbonation rate K(mm/(yrs)$^{1/2}$)		
				Mean Value μ_{x_0}	Standard Deviation σ_{x_0}	Varience δ_{x_0}	Mean Value μ_k	Standard Deviation σ_k	Varience δ_k
A	1949	49	6	12.77	7.122	0.5579	1.824	1.017	0.5579
B	1978	20	20	19.30	23.060	1.1950	4.314	5.157	1.1950
C	1972	26	6	7.55	8.155	1.0800	1.481	1.599	1.0800
D	1980	18	12	12.79	9.989	0.7809	3.015	2.355	0.7809
E	1972	26	8	19.31	19.980	0.9310	3.788	3.526	0.9310
F	1983	15	18	13.51	9.671	0.7158	3.489	2.497	0.7158
G	1974	24	20	10.37	9.323	0.8995	2.116	1.903	0.8995
H	1984	14	10	10.70	10.760	1.006	2.860	2.876	1.0060
I	1974	24	20	14.77	11.250	0.7620	3.015	2.359	0.7824

*: A—Huey-tong bridge, B—Beei-men viaduct, C—Way-shuang vivulet bridge, D—her-pyng west road viaduct, E—Jzyh-chyang bridge, F—Ay-gwo west road viaduct, G—old Hwan-nan viaduct, H—Daw-nan bridge and I—Shi-yuan bridge

Table 3

The fact to be noted in Table 3 is the high standard deviation of K. In all cases, the mean μ_K and standard deviation σ_K are nearly equal, with σ_K exceeding μ_K in a few cases. If the variability of K were modeled as a normal distribution, it would be possible to obtain negative values with a high probability. Here we model K as

$$K = \gamma_C \cdot \overline{K} \cdot \varepsilon_L \tag{17}$$

where γ_C is a scale factor that accounts for the increase of the carbon dioxide concentration above atmospheric levels within a parking structure, $\overline{K}$ is the carbonation rate coefficient, assumed to be constant for a given concrete parking structure, but varies between structures, and ε_L is a log-normal random variable, with expected value one, that accounts for variations of K within a given structure.

To quantify the variability of $\overline{K}$ and ε_L, we use the data compiled by Liang et al. (2001). The first step is to calculate the mean and standard deviation for $\overline{K}$. The mean carbonation rate coefficient, $\mu_{\overline{K}}$, is taken as the weighted average of μ_K for each structure, given in Table 4, with weighting factor proportional to the number of test points, n. The standard deviation, $\sigma_{\overline{K}}$, is then calculated from Equation (19). The data for bridges A and C were excluded from all analyses because of the low number of test points for these bridges.

$$\mu_{\overline{K}} = \frac{\sum n_i \cdot \mu_{K,i}}{\sum n_i} = 3.21 \ \frac{mm}{yr^{1/2}} \tag{18}$$

$$\sigma_{\overline{K}} = \sqrt{E(\mu_K^2) - \left(E(\mu_K)\right)^2} = 0.713 \tag{19}$$

The result is $\overline{K}$ is normally distributed with mean 3.21 and standard deviation 0.713. The probability density function of $\overline{K}$ is shown in Figure 2.

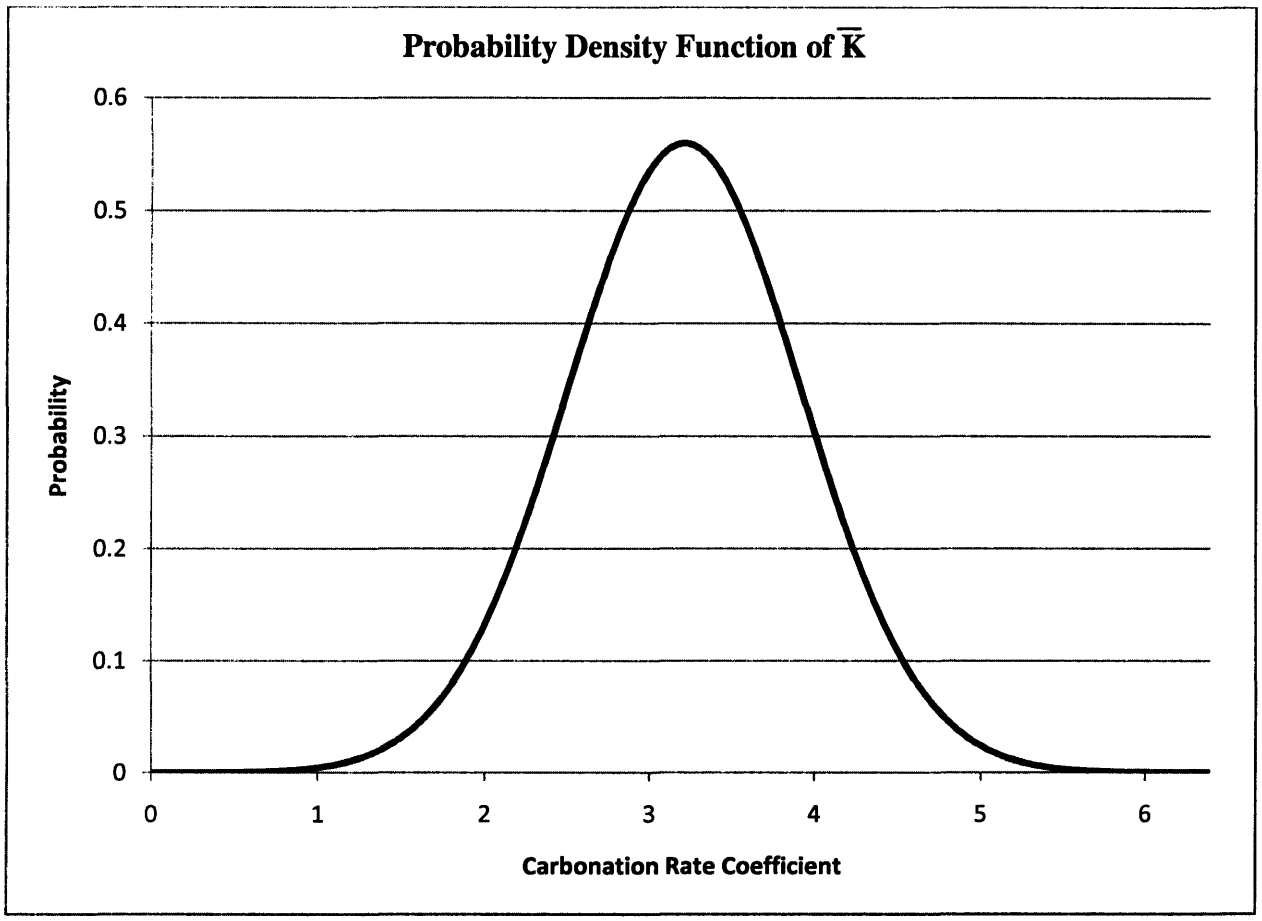

Figure 2

The next step is to establish the mean and standard deviation for ε_L. We first take the data compiled by Liang et al. (2001) and scale the distributions so they have a mean of one. This step is necessary to insure that ε_L has an expected value of one. The mean and standard deviation of the moments of ε_L are denoted $\mu_{\varepsilon L}$ and $\sigma_{\varepsilon L}$. Next, the mean $\mu_{LN(\varepsilon L)}$ and standard deviation $\sigma_{LN(\varepsilon L)}$ of $\ln(\varepsilon_L)$ are calculated from

$$\mu_{LN(\varepsilon L)} = 2\ln(\mu_{\varepsilon L}) - \frac{1}{2}\ln(\sigma_{\varepsilon L}^2 + \mu_{\varepsilon L}^2) \tag{20}$$

$$\sigma_{LN(\varepsilon L)}^2 = -2\ln(\mu_{\varepsilon L}) + \ln(\sigma_{\varepsilon L}^2 + \mu_{\varepsilon L}^2) \tag{21}$$

where $\mu_{\varepsilon L}$ and $\sigma_{\varepsilon L}$ are the mean and standard deviation of ε_L for each bridge and $\mu_{LN(\varepsilon L)}$ and $\sigma_{LN(\varepsilon L)}$ are the mean and standard deviation of the natural-log of ε_L for each bridge. This process is shown in Table 4 below.

	Empirical Moments		Moments of $\varepsilon_L = K/\mu_K$		Moments of $\ln(\varepsilon_L)$	
Bridge	μ_K	σ_K	$\mu_{\varepsilon L}$	$\sigma_{\varepsilon L}$	$\mu_{LN(\varepsilon L)}$	$\sigma_{LN(\varepsilon L)}$
B	4.314	5.157	1	1.195	-0.444	0.942
D	3.015	2.355	1	0.781	-0.238	0.690
E	3.788	3.526	1	0.931	-0.312	0.790
F	3.489	2.497	1	0.716	-0.207	0.643
G	2.116	1.903	1	0.899	-0.296	0.770
H	2.860	2.876	1	1.006	-0.349	0.836
I	3.015	2.359	1	0.782	-0.239	0.691

Table 4

The last step is to find the average of $\mu_{LN(\varepsilon L)}$ and $\sigma_{LN(\varepsilon L)}$. The result is $\ln(\varepsilon_L)$ is normally distributed with mean -0.298, standard deviation of 0.765, and expected value 1.

The probability density function of ε_L is shown in Figure 3.

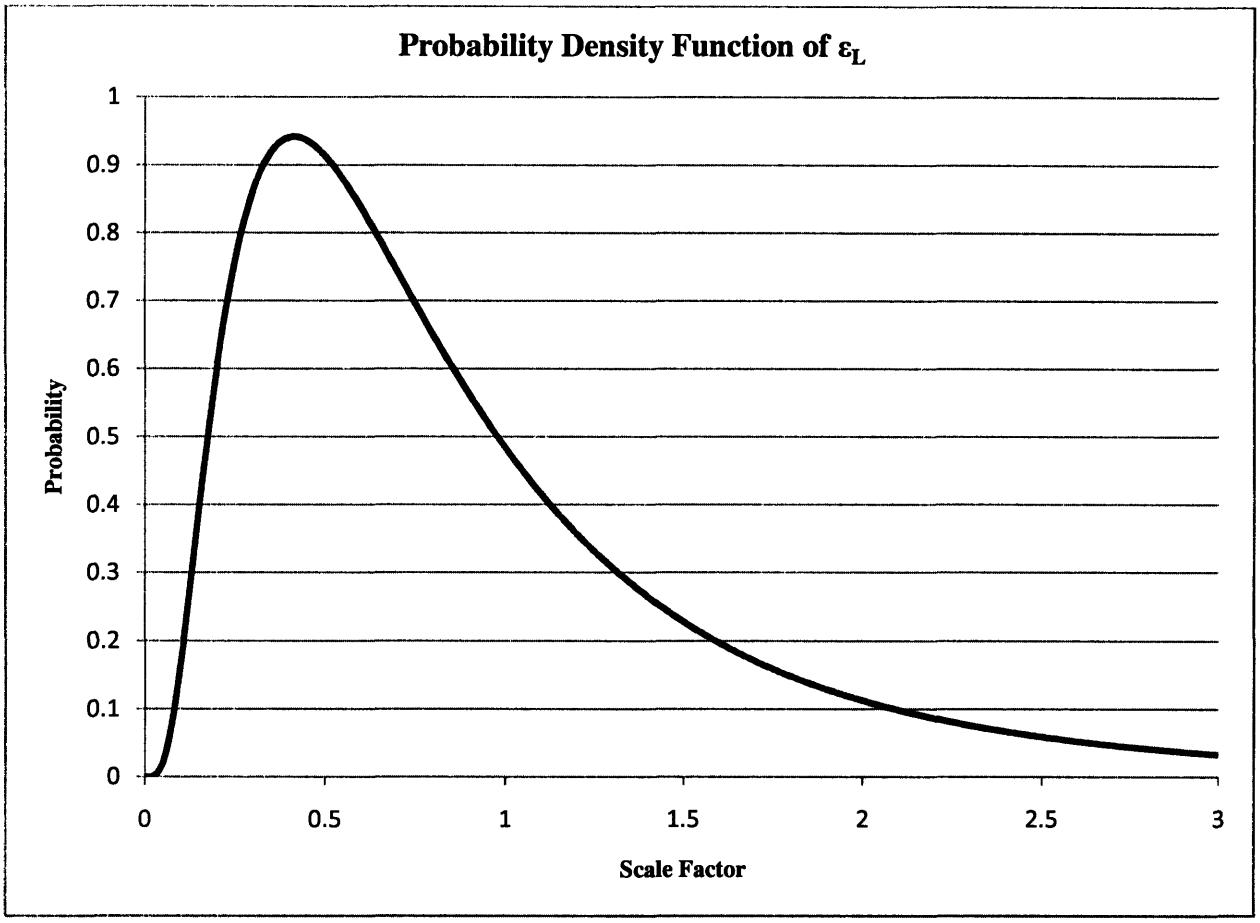

Figure 3

4.2 DETERMINING γ_C

As mentioned previously, to accurately model the carbonation of concrete in parking structures, the microclimate created by the increased carbon dioxide concentration needs to be accounted for. In the present model, this environmental factor is called γ_C and represents the percent increase over atmospheric carbon dioxide concentrations; for example, $\gamma_C = 1.25$ corresponds to a 25-percent increase in the parking structure concentration of carbon dioxide. The environmental factor was calculated this way because the models developed previously were based on observations from bridges and other marine structures, i.e. structures that only experience carbonation from atmospheric carbon dioxide. These types of structures are already subject to atmospheric CO_2 concentrations, which results in models that already include carbonation of the structural elements from atmospheric CO_2. As a result, γ_C can be thought of as increasing the CO_2 source concentration above atmospheric levels. In addition, γ_C needs to be calculated for each level of a parking structure because the number of cars passing through a given level decreases for each level after level one. The procedure for calculating γ_C is now presented.

1) Estimate number of cars per day: N_C
    a. This may be determined from traffic counts taken for a specific structure or determined by an analytical method. An example analytical method is presented in Appendix A.

2) Calculate the number of car per level: $N_i = \frac{N_C}{N}$, where i ranges from one to N.
   a. N_i – Number of cars per day on the i^{th} level
   b. N_C – Total number of cars per day for the structure
   c. N – Number of levels in the structure
   d. This number will be equal for all levels

3) Calculate cumulative number of cars per day for each level: $CN_j = \sum_{i=j}^{N} N_i$, where j ranges from one to N. CN_j is the cumulative number of cars per day on the j^{th} level.

4) Calculate travel length of a car, in miles, for each level of structure: L
   a. Can be assumed equal to centerline length of driveline
   b. Typically the same for each level

5) Calculate amount of CO2 emitted on each level: $C_i = \frac{(L_i \cdot 1.2)(CN_i)}{V_i}$, where i ranges from 1 to N.
   a. C_i – Concentration of CO_2 from vehicle emissions on the ith level (lb/ft^3)
   b. L_i – Length car travels through the i^{th} level
   c. 1.2 – Amount of carbon dioxide emitted by the average car (lb/mi)
   d. CN_i – Cumulative number of cars for the i^{th} level
   e. V_i – Volume of the i^{th} level in cubic feet

6) Calculate γ_C: $\gamma_{C,i} = 1 + \frac{C_i}{4.6 \cdot 10^{-5}}$ (22)
   a. $\gamma_{C,i}$ – Increased CO_2 concentration for the i^{th} level
   b. C_i – CO_2 concentration from vehicle emissions on the i^{th} level (lb/ft^3)
   c. $4.6x10^{-5}$ – Atmospheric concentration of CO_2 (lb/ft^3)

After examining the final form of Equation (22), it is clear that $\gamma_C = 1$ would represent no increase in CO_2 concentration above atmospheric levels. It is acceptable to choose $\gamma_C = 1$ for the top level of a typical parking structure. (It should be noted that the roof levels of parking structures deteriorate in significantly different ways than the rest of the structure. Rain water dramatically speeds the process of chloride ingress into concrete surfaces, particularly when it is allowed to pond on concrete surfaces. This type of deterioration is not considered here, but must be considered when performing service life predictions of concrete parking structures.)

4.3 DETERIORATION CURVES

Finally, the deterioration model needs to be converted into a form that is suitable for comparing the maintenance and repair strategies that will be introduced in the next section. While it is sufficient to know the depth of carbonation at a given time, it is much more useful to know the percentage of a structure with a given depth of carbonation at a given time. A series of curves can then be generated for different values of $\gamma_C \overline{K}$. The process for developing these curves begins by writing the above deterioration criteria as an equation,

$$F_D(t) = Fraction\ of\ structure\ with\ X_0 \geq X^* \quad (23)$$

where X_O is the depth of carbonation and X* is the depth at which carbonation begins to initiate deterioration, typically taken as the depth of the steel reinforcement. As discussed in the Introduction, the carbonation front must reach the depth of the steel reinforcement before corrosion can initiate. Substituting Equation (16) for X_O, Equation (17) for K and solving for ε_L gives

$$F_D(t) = P\left[\varepsilon_L \geq \frac{X^*}{\gamma_C \cdot \overline{K} \cdot \sqrt{t}}\right] \tag{24}$$

The right hand side of Equation (24) is one minus the cumulative distribution function (CDF) for ε_L. Taking X* = 40-mm and $\gamma_C = 1$, Figure 4 plots the fraction deteriorated against time for different values of $\overline{K}$.

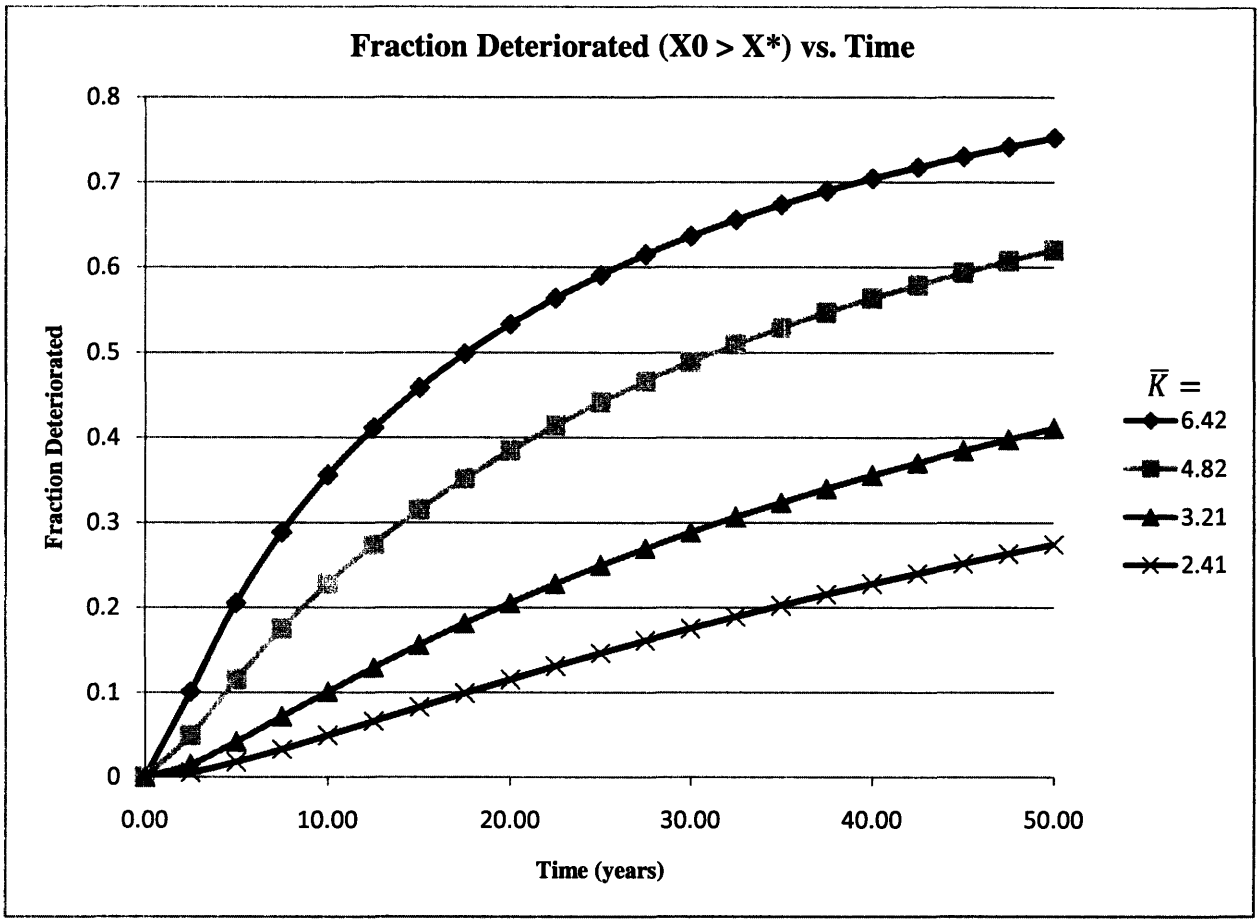

Figure 4

CHAPTER 5: ECONOMIC COMPARISON OF MAINTENANCE PROGRAMS

Concrete deterioration in parking structures is almost exclusively limited to floor slabs. This is due to a number of factors, including water ponding and vehicular traffic. A variety of methods to repair and prevent deterioration of concrete slabs have been developed during the past few decades. To repair concrete structures spalled concrete is removed by jackhammer, the corroded reinforcing steel is cleaned, and new concrete placed. Repair mortars that contain corrosion inhibiting admixtures may be used in lieu of plain concrete to repair spalled areas.

To prevent deterioration, two types of surface treatments have been developed: penetrating sealers and waterproofing membranes. Penetrating sealers are water or petroleum based liquids that fill the pores of a concrete slab and slow the ingress of carbon dioxide. Recent studies (Ibrahim et al. 1999) have shown penetrating sealers can only reduce the rate of carbonation, they cannot stop it completely. Waterproofing membranes, however, sit on stop of the concrete substrate and prevent any carbonation of the concrete below them.

These techniques for maintaining concrete parking structures have been in use for some time, but studies to quantify the economic benefit, or cost, of preventative maintenance have not been conducted. To correct this deficiency, a cost-analysis of four different maintenance programs will be performed to determine if there is an economically optimal strategy for repair and maintenance of concrete parking structures.

5.1 MAINTENANCE PROGRAMS

Using the concrete deterioration model developed in Chapter 4, the maintenance programs described in Table 5 will be investigated to determine which one provides the greatest present worth from revenues and costs. These strategies are adaptations of programs suggested by Chrest et al. (2001) and are based on the repair and prevention methods previously mentioned in this chapter.

Program Name	Description	Effect on $\overline{K}$
No Prevention	No preventative measures taken; repair concrete as required	No change
Normal Prevention	Apply penetrating sealer every 5 years; repair concrete as required	Initial reduction but benefit decreases with time
Conservative Prevention	Apply penetrating sealer every year; repair concrete as required	Constant reduction
Extreme Prevention	Apply waterproofing membrane every 5 years	Waterproofing membrane stops carbonation of concrete; no repairs required

Table 5

5.2 LIFETIME CURVES

To determine the repair costs and revenue generated over the life of a concrete parking structure the lifetime curve for the structure must be established. The lifetime curves are based on the deterioration curves developed in Chapter 4 and at each time give the fraction of deteriorated floor slabs including the effects of repairs and maintenance actions. To create the deterioration curve for a concrete structure, the environmental factors, γ_C for each level, and average carbonation rate coefficient, $\overline{K}$ for the structure, must be known and the critical depth of carbonation, X*, must be estimated. After finding the deterioration curve, the lifetime curve can be determined by specifying two additional parameters: the critical fraction deteriorated, F_D*, and the fraction repaired, F_R. The critical fraction deteriorated is the fraction of the ramp that must deteriorate in order to trigger a repair. The fraction repaired is the amount of material removed during a repair, and is typically greater than or equal to the fraction deteriorated. For this study, F_D* is taken as 0.05 or 0.10 and F_R is specified as a multiple of F_D*, $F_R = \{1.0F_D^*, 1.5F_D^*, 2.0F_D^*\}$. All combinations of F_D* and F_R will be considered for each maintenance program.

After selecting a combination of F_D* and F_R, the lifetime curve for a particular maintenance program can be found. The first step is to establish the deterioration curve for each maintenance program based on the effect the program has on the value of $\overline{K}$ for a structure. For the "No Prevention" program $\overline{K}$ is not changed and the "Conservative Prevention" program is assumed to reduce $\overline{K}$ to half its value. In the "Normal Prevention" program the sealer is applied once every five years and $\overline{K}$ is not constant: after initially decreasing to half its original value, the carbonation rate coefficient is assumed to increase linearly to the full value of $\overline{K}$ is reached inthe year before another application of the penetrating sealer. Figures 5, 6, and 7 show deterioration curves with $\gamma_C = 1.0$ and $\overline{K} = 3.21\ mm/yr^{1/2}$ for the three cases discussed above. The fourth case, "Extreme Prevention," does not need a deterioration curve because deterioration does not occur when a waterproofing membrane is applied.

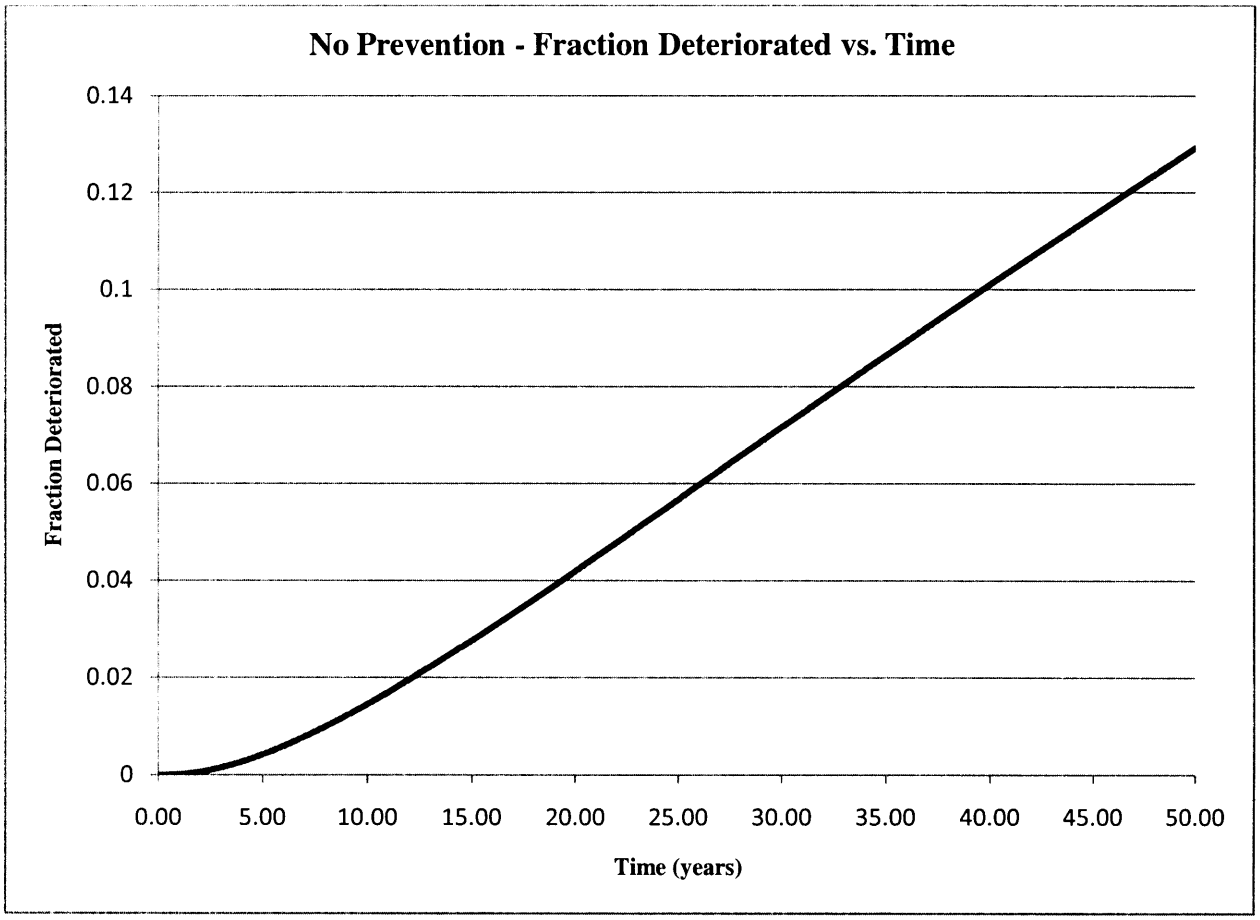
No Prevention - Fraction Deteriorated vs. Time
Fraction Deteriorated
0.14
0.12
0.1
0.08
0.06
0.04
0.02
0
0.00
5.00
10.00
15.00
20.00
25.00
30.00
35.00
40.00
45.00
50.00
Time (years)

Figure 5

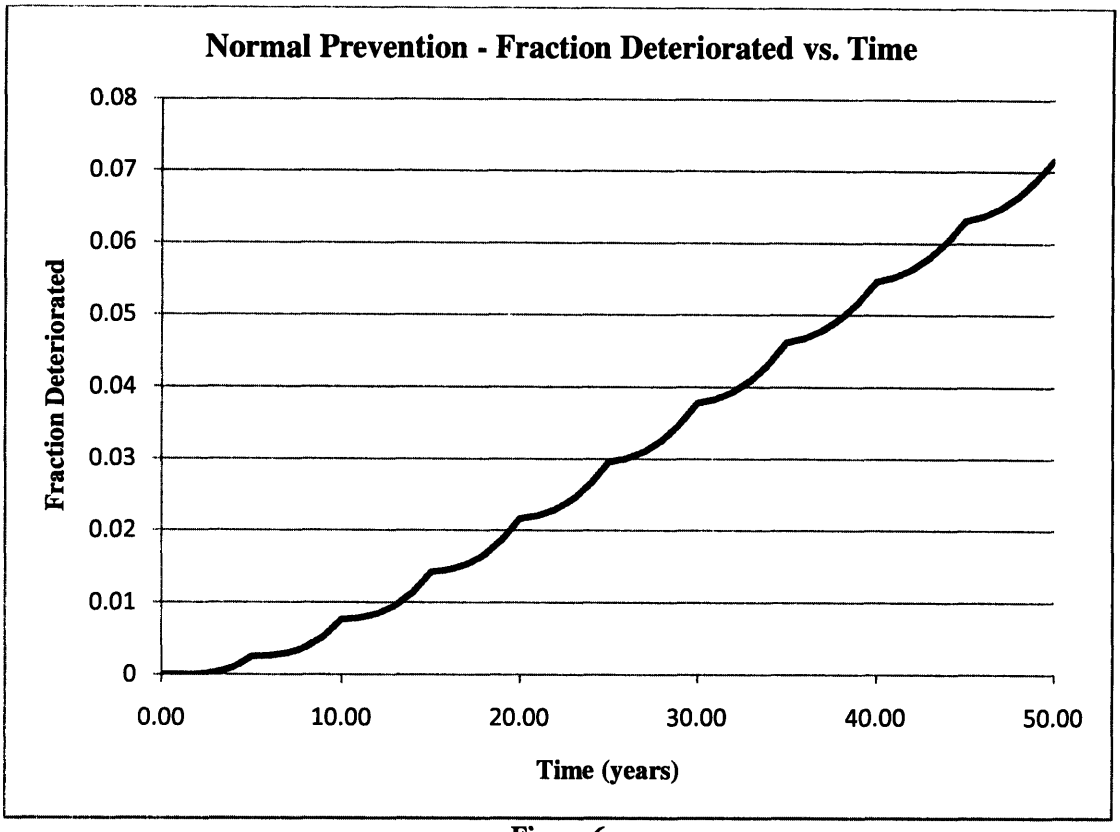

Figure 6

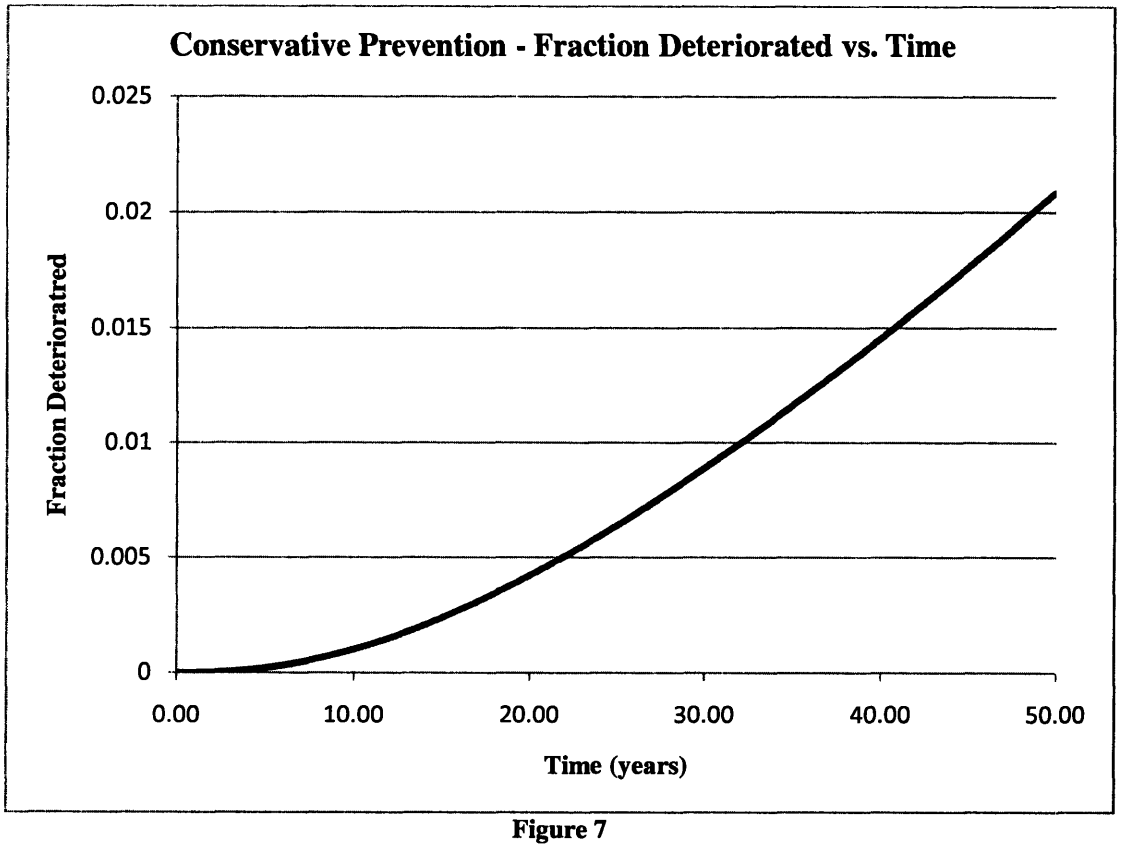

Figure 7

Next, the times at which the structure is repaired are found. The time to first repair, t_1, is simply the time when the deterioration curve, $F_D^0(t)$, equals F_D^*. After finding t_1, the offset time t_1', a result of taking F_R greater than F_D^*, is found; if F_R equals F_D^* then t_1' equals t_1. This process is shown in Figure 8.

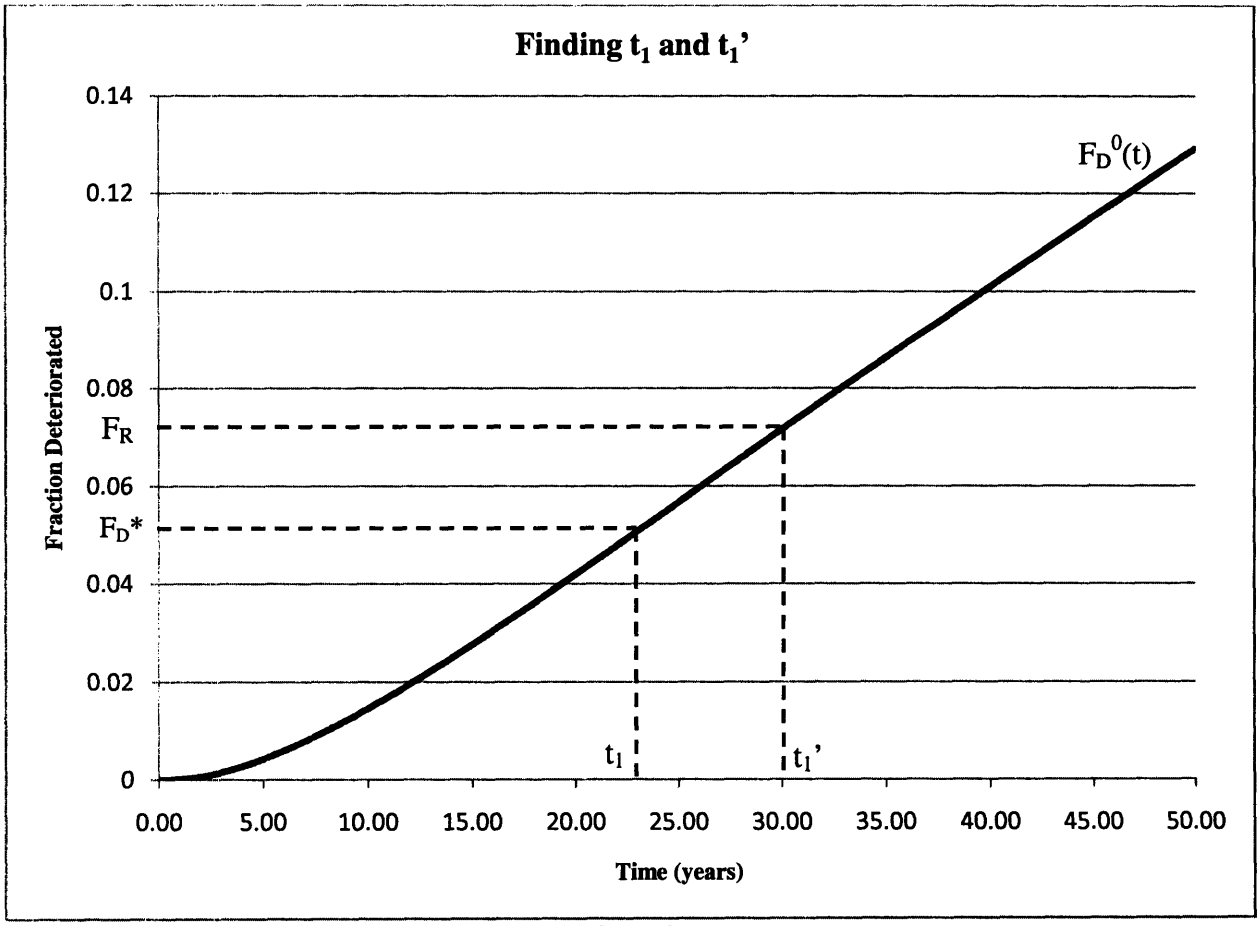

Figure 8

Next, the deterioration of the parking structure starting at t_1 is calculated. After repair, at time t1 a fraction F_R of the structure is new material and has zero deterioration, while the remaining structure, $1 - F_R$, is partially deteriorated. Thus, the deterioration curve after t_1, $F_D^1(t)$, has two components: the first component is $F_R \cdot F_D^0(t)$ and begins at t_1. The second component is zero up to t1' and equals $F_D^0(t) - F_R$ for $t > t_1'$. Summing the two components gives the deterioration curve $F_D^1(t)$ for times greater than t_1. Figure 9 shows $F_D^1(t)$ and its components.

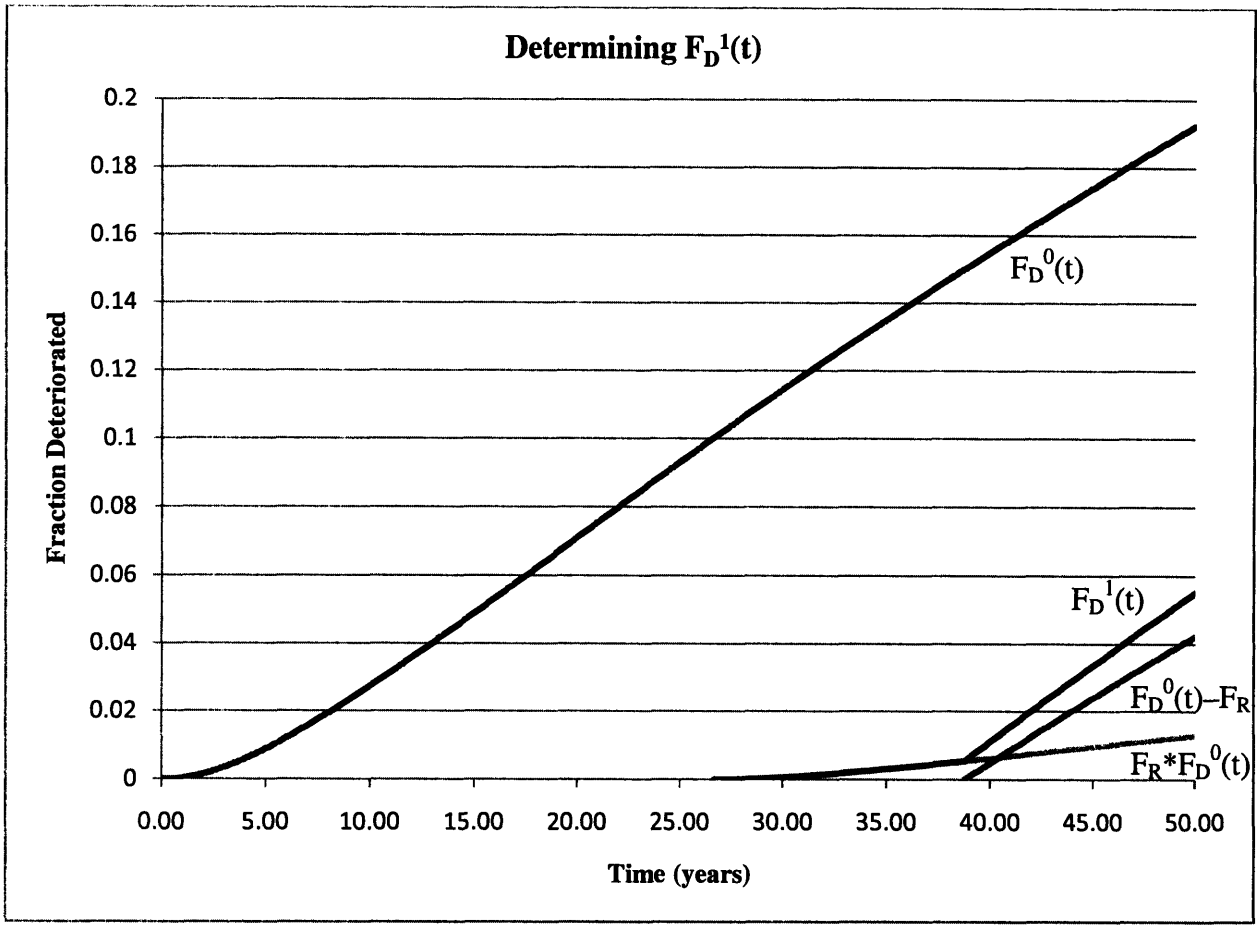

Figure 9

Next, the time to second repair and second offset time, t_2 and t_2' respectively, are found from deterioration curve $F_D^1(t)$. Using these times, $F_D^2(t)$ is determined in the same way as $F_D^1(t)$; however, $F_D^2(t)$ has three components. The first component is $F_R \cdot F_D^0(t)$, beginning at t_2, and represents the deterioration of the new material placed at time t_2. To find the second and third components of $F_D^2(t)$, we use the curves that were added to find $F_D^1(t)$. When the repair at time t_2 is made, a portion of F_R comes from $F_R \cdot F_D^0(t)$ and the remainder comes from $F_D^0(t) - F_R$. By drawing a vertical line on the deterioration curve at t_2', where $F_D^1(t)$ equals F_R, the fraction repaired that comes from each component is found. Shifting these curves down by the contribution each makes to F_R yields the second and third components of $F_D^2(t)$, which account for the fraction of the structure that is partially deteriorated. This process continues, increasing the number of components of the deterioration curve by one after each repair, until the design life of the structure is reached. In this study, the design life is taken as 50 years for all maintenance programs. The lifetime curve for a given structure and maintenance program is the combination of the deterioration curves, $F_D^0(t)$, $F_D^1(t)$, etc, each applying over different time periods, $(0, t_1)$, (t_1, t_2), etc. An example lifetime curve is shown in Figure 10.

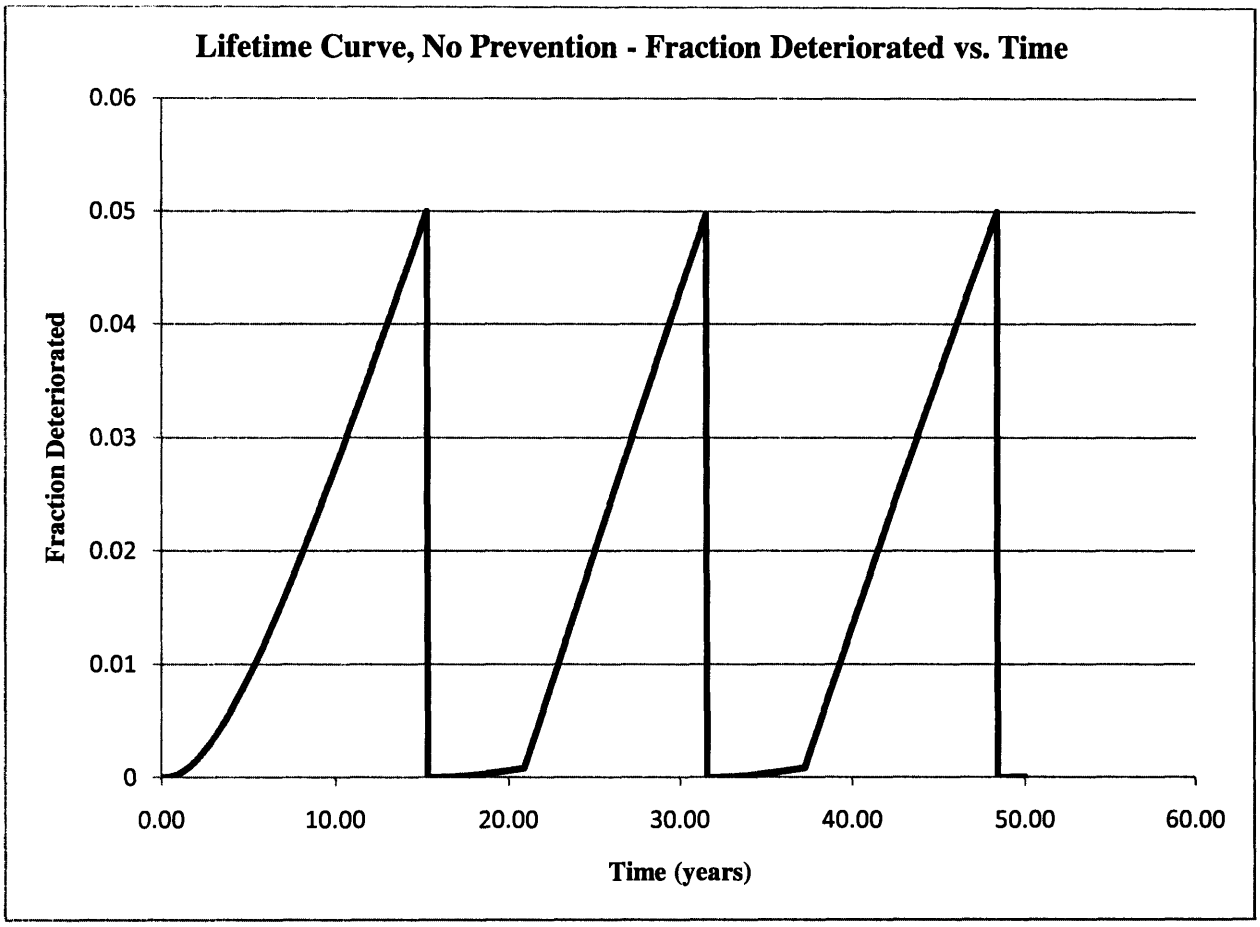

Figure 10

5.3 ECONOMIC ANALYSIS

After finding the lifetime curves and repair times, the revenue and costs for each maintenance program are quantified by applying each maintenance program to one level of a fictitious parking ramp (we consider only one level because the environmental factor varies between levels). The ramp for this study has a surface area of 40,000 SF per level, which equates to about 175 parking stalls and a monthly revenue of $30,000 when the full capacity of the level is available for parking. The procedures for calculating the revenue and costs for each maintenance program are discussed below.

REVENUE – The monthly revenue produced by a parking structure is directly proportional to the fraction of the structure open for parking. The fraction for parking decreases as the structure deteriorates because deteriorated areas are unsafe to use and drivers will be increasingly reluctant to use a structure that shows signs of deterioration. The revenue earned as a function of time, R(t), is assumed to be

$$R(t) = E_0[1 - 3 \cdot F_D(t)] \tag{25}$$

where E_0 is the revenue of the level at full capacity, taken as $30,000 per month for this study, and $F_D(t)$ is the fraction of the structure deteriorated at time t. $F_D(t)$ is multiplied by a factor of 3 to account for decreased safety and traffic volume due to deterioration of a structure.

CONCRETE REPAIR COST – Concrete repair costs are calculated from the fraction of the level repaired, F_R, and the unit cost of the repair, taken as \$45 per square foot. In addition, a fixed cost is added to the cost of the repairs each time a repair is required (in the construction sector this cost is called mobilization cost). The total concrete repair cost for one repair, C_C, is expressed as

$$C_C = \$10{,}000 + \$45.00(F_R \cdot A) \tag{26}$$

where A is the surface area of one level of the concrete parking structure, 40,000 square feet for this study.

PENETRATING SEALER AND WATERPROOFING MEMBRANE COSTS – Costs for penetrating sealer and waterproofing membrane are calculated in a way similar to the concrete repair cost. However, the mobilization cost is lower since penetrating sealers and waterproofing membranes require much less equipment than concrete repairs; the unit costs are also different. In addition, sealers and membranes are applied to the entire level, so F_R is not needed. The expression we use for penetrating sealer cost per application, C_S, and waterproofing membrane cost per application, C_M, are

$$C_S = \$5{,}000 + \$0.50 \cdot A \tag{27}$$

and

$$C_M = \$5{,}000 + \$4.00 \cdot A \tag{28}$$

The final step is to convert the revenue generated and costs incurred to present worth values so the maintenance programs may be compared. The present worth P of a single payment F made at time t is taken to be

$$P = Fe^{-it} \tag{29}$$

where i is the discount rate, taken as 3% per year for this study. Equation (29) is used to find the present worth of revenue and concrete repair, penetrating sealer, and waterproofing membrane costs. The net present worth for each maintenance program is then calculated by summing the present worth contribution from each discrete time period.

5.4 RESULTS AND DISCUSSION

To compare the economic benefit of the maintenance programs, lifetime curves were generated for each maintenance program for large and small values of $\gamma_C \overline{K}$. For the small values, γ_C was taken as 1 and $\overline{K} = \{2.50, 3.21, 3.92\}$; for the large value, $\gamma_C = 2$ and $\overline{K} = 4.00$. The fraction deteriorated and fraction repaired parameters were also varied to determine what effect they have on the present worth of a parking structure. The results of these simulations are presented in Tables 6 – 9. The net present worth of the optimum strategy in each table is shown in boldface print.

γ_c	2.5					
Fraction Deteriorated	0.05			0.1		
Fraction Repaired	0.05	0.075	0.10	0.1	0.15	0.20
No Prevention						
Revenue	$8,900	$8,938	$8,938	$8,718	$8,718	$8,718
Repair Cost	($32)	($47)	($62)	$0	$0	$0
Net Present Worth	*$8,868*	***$8,891***	*$8,876*	*$8,718*	*$8,718*	*$8,718*
Normal Prevention						
Revenue	$9,025	$9,025	$9,025	$9,025	$9,025	$9,025
Sealer Cost	($145)	($145)	($145)	($145)	($145)	($145)
Repair Cost	$0	$0	$0	$0	$0	$0
Net Present Worth	*$8,880*	*$8,880*	*$8,880*	*$8,880*	*$8,880*	*$8,880*
Conservative Prevention						
Revenue	$9,253	$9,253	$9,253	$9,253	$9,253	$9,253
Sealer Cost	($663)	($663)	($663)	($663)	($663)	($663)
Repair Cost	$0	$0	$0	$0	$0	$0
Net Present Worth	*$8,591*	*$8,591*	*$8,591*	*$8,591*	*$8,591*	*$8,591*
Extreme Prevention						
Revenue	$9,311	$9,311	$9,311	$9,311	$9,311	$9,311
Membrane Cost	($957)	($957)	($957)	($957)	($957)	($957)
Net Present Worth	*$8,354*	*$8,354*	*$8,354*	*$8,354*	*$8,354*	*$8,354*

Note: Amounts shown in thousands of dollars

Table 6

$\gamma_C \bar{K}$	3.21					
Fraction Deteriorated	0.05			0.1		
Fraction Repaired	0.05	0.075	0.10	0.1	0.15	0.20
No Prevention						
Revenue	$8,796	$8,878	$8,942	$8,437	$8,477	$8,476
Repair Cost	($81)	($108)	($96)	($58)	($85)	($113)
Net Present Worth	*$8,715*	*$8,769*	***$8,847***	*$8,379*	*$8,392*	*$8,364*
Normal Prevention						
Revenue	$8,888	$8,921	$8,921	$8,717	$8,717	$8,717
Sealer Cost	($145)	($145)	($145)	($145)	($145)	($145)
Repair Cost	($32)	($46)	($60)	$0	$0	$0
Net Present Worth	*$8,711*	*$8,730*	*$8,716*	*$8,572*	*$8,572*	*$8,572*
Conservative Prevention						
Revenue	$9,166	$9,166	$9,166	$9,166	$9,166	$9,166
Sealer Cost	($663)	($663)	($663)	($663)	($663)	($663)
Repair Cost	$0	$0	$0	$0	$0	$0
Net Present Worth	*$8,504*	*$8,504*	*$8,504*	*$8,504*	*$8,504*	*$8,504*
Extreme Prevention						
Revenue	$9,311	$9,311	$9,311	$9,311	$9,311	$9,311
Membrane Cost	($957)	($957)	($957)	($957)	($957)	($957)
Net Present Worth	*$8,354*	*$8,354*	*$8,354*	*$8,354*	*$8,354*	*$8,354*

Note: Amounts shown in thousands of dollars

Table 7

$\gamma_C \bar{K}$	3.92					
Fraction Deteriorated	0.05			0.1		
Fraction Repaired	0.05	0.075	0.10	0.1	0.15	0.20
No Prevention						
Revenue	$8,730	$8,861	$8,948	$8,222	$8,482	$8,535
Repair Cost	($164)	($182)	($183)	($128)	($126)	($166)
Net Present Worth	*$8,566*	*$8,679*	***$8,765***	*$8,095*	*$8,356*	*$8,369*
Normal Prevention						
Revenue	$8,824	$8,834	$8,973	$8,437	$8,443	$8,443
Sealer Cost	($145)	($145)	($145)	($145)	($145)	($145)
Repair Cost	($74)	($107)	($90)	($49)	($73)	($96)
Net Present Worth	*$8,605*	*$8,581*	*$8,738*	*$8,243*	*$8,225*	*$8,202*
Conservative Prevention						
Revenue	$9,028	$9,028	$9,028	$9,028	$9,028	$9,028
Sealer Cost	($663)	($663)	($663)	($663)	($663)	($663)
Repair Cost	$0	$0	$0	$0	$0	$0
Net Present Worth	*$8,365*	*$8,365*	*$8,365*	*$8,365*	*$8,365*	*$8,365*
Extreme Prevention						
Revenue	$9,311	$9,311	$9,311	$9,311	$9,311	$9,311
Membrane Cost	($957)	($957)	($957)	($957)	($957)	($957)
Net Present Worth	*$8,354*	*$8,354*	*$8,354*	*$8,354*	*$8,354*	*$8,354*

Note: Amounts shown in thousands of dollars

Table 8

$\gamma_C \bar{K}$	8.00					
Fraction Deteriorated	0.05			0.1		
Fraction Repaired	0.05	0.075	0.10	0.1	0.15	0.20
No Prevention						
Revenue	$8,655	$8,857	$8,931	$8,013	$8,361	$8,452
Repair Cost	($985)	($769)	($799)	($671)	($719)	($773)
Net Present Worth	*$7,670*	*$8,088*	*$8,132*	*$7,342*	*$7,642*	*$7,679*
Normal Prevention						
Revenue	$8,671	$8,855	$8,942	$8,082	$8,381	$8,477
Sealer Cost	($145)	($145)	($145)	($145)	($145)	($145)
Repair Cost	($435)	($439)	($473)	($357)	($402)	($408)
Net Present Worth	*$8,091*	*$8,271*	*$8,324*	*$7,580*	*$7,834*	*$7,924*
Conservative Prevention						
Revenue	$8,734	$8,866	$8,949	$8,232	$8,467	$8,541
Sealer Cost	($663)	($663)	($663)	($663)	($663)	($663)
Repair Cost	($170)	($186)	($188)	($133)	($130)	($172)
Net Present Worth	*$7,902*	*$8,017*	*$8,098*	*$7,436*	*$7,675*	*$7,706*
Extreme Prevention						
Revenue	$9,311	$9,311	$9,311	$9,311	$9,311	$9,311
Membrane Cost	($957)	($957)	($957)	($957)	($957)	($957)
Net Present Worth	***$8,354***	***$8,354***	***$8,354***	***$8,354***	***$8,354***	***$8,354***

Note: Amounts shown in thousands of dollars

Table 9

The net present worth values follow the same pattern. For a given $\gamma_C \overline{K}$ and F_D*, the present worth values increase as the fraction repaired is increased. However, the increase is much larger when stepping from F_R=F_D* to F_R=1.5F_D* than from F_R=1.5F_D* to F_R=2.0F_D*. This indicates there may be a single optimum combination of F_D* and F_R. It is also noted that the net present worth for programs with $F_D^* = 0.05$ is larger than the net preset worth of programs with $F_D^* = 0.10$ for all values of $\gamma_C \overline{K}$. This indicates that choosing an appropriate deterioration threshold for concrete repairs is important in maximizing the net present worth of a parking structure.

The revenue for each maintenance program generally follows the same pattern as the net present worth, increasing with the fraction repaired. However, there are two exceptions that are observed. First, in Table 6 the "No Prevention" revenue does not change when the fraction repaired is increased from 0.075 to 0.10. Similarly, the revenue for the "Normal Prevention" program in Table 7 does not change when F_R increases from 0.075 to 0.10. This does not make sense because the purpose of taking $F_R > F_D$* is to produce a time period with a slower rate of deterioration, which should result in greater revenue. The discrepancy is the result of the final concrete repair being made very close to the end of the design life of the structure. For these cases where F_R=0.075, the repair is so close to the end that the period of slower deterioration reaches the design life. For F_R=0.10, the repair occurred at an earlier time, which resulted in the deterioration curve reaching its full deterioration rate before reaching the design life. (The change in deterioration rate is shown in Figure 9, curve $F_D^1(t)$.

The net present worth also indicates that a single maintenance program does not maximize the net present worth for all values of $\gamma_C \overline{K}$. In Tables 7 and 8, which correspond to lower values of $\gamma_C \overline{K}$, the "No Prevention" program produces slightly higher net present worth values than the "Normal Prevention" program and significantly higher values than the "Conservative Prevention" and "Extreme Prevention" programs. Conversely, Table 9 reveals that for higher values of $\gamma_C \overline{K}$ the "Extreme Prevention" program yields the largest net present worth. This change indicates that the optimum maintenance strategy for a parking structure will require different maintenance programs for different levels. "Extreme Prevention" is the most economical choice for the lower levels of a parking structure where $\gamma_C \overline{K}$ is the largest and "Normal Prevention" or "No Prevention" for the upper levels where $\gamma_C \overline{K}$ is smaller.

CHAPTER 6: CONCLUSIONS

In this study, a carbonation model for concrete parking structures was developed. The model was used to analyze several maintenance programs to determine the most economic way to repair and maintain concrete parking structures. For structures that have low carbonation resistance, $\gamma_C \overline{K} \geq 8.00$, applying a waterproofing membrane every five years is the most economical way to prevent deterioration of the structure. For structures with high resistance, $\gamma_C \overline{K} \leq 3.21$, repairing the concrete as required is the best economic solution; no prevention is required. When this strategy is used, the structure should be repaired when approximately 5% of the structure shows signs of deterioration. In practice, a combination of the repair and prevention methods presented in this study will produce an optimal maintenance program. For example, the lowest levels of a parking structure will have significantly higher γ_C than the upper levels due to higher traffic volumes at the lower levels. This leads to an optimal maintenance program that uses waterproofing membrane at the lower levels, but switches to penetrating sealer for the upper floors.

In this study, a large number of parameters were identified that affect how quickly a structure deteriorates over time. These include carbonation rate coefficient, cover over steel reinforcement, and environmental factor γ_C. Approximations for $\overline{K}$ and γ_C were developed in this study, but the variability in the depth of the reinforcing steel was ignored. Small variations in the depth of the steel could have a large impact on the fraction of a concrete structure repaired, which directly affects the proper maintenance program for the structure. In addition, the variability in $\overline{K}$ for parking structures needs to be further researched so more accurate models may be developed. The probability distribution describing $\overline{K}$ in this study is based on data obtained from bridges, which do not accurately reflect the microclimate created within a parking structure. A more accurate method for determining γ_C would also be useful.

Further, sensitivity analyses of the net present worth need to be conducted. In general, the differences in present worth between different maintenance programs are not that large and small changes in the unit costs for concrete repair and sealer and membrane application could alter the results. It would also be appropriate to perform additional simulations to find the optimum values of F_D* and F_R for repair and see how these parameters vary for different levels of carbonation resistance, different microclimates, and different economic parameters.

REFERENCES

Amey, S.L., Johnson, D. A., Miltenberger, M.A., and Farzam, H. (1998). "Temperature dependence of compressive strength of conversion-inhibited high alumina cement concrete." *ACI Structural Journal*, 95(1), 27 – 36.

Baluch, M.H., Rahman, M.K., Al-Gadhib, A.H. (2002). "Risks of cracking and delamination in patch repair." *Journal of Materials in Civil Engineering*, ASCE, 14(4), 294 – 302.

Bazant, Z.P. (1979b). "Physical model for steel corrosion in concrete sea structures – application." *Journal of the Structural Division,* ASCE, 105(6), 1155 – 1166.

Branco, F.J.F.G., Tadeu, A.J.B., Nogueira, J.A.D. (2003). "Bond geometry and shear strength of steel plates bonded to concrete on heating." *Journal of Materials in Civil Engineering*, ASCE, 15(6), 586 – 593.

Campbell, D.H., Sturm, R.D., Kosmatka, S.H. (1991). "Detecting Carbonation." *Concrete Technology Today*, PCA, 12(1), 1 – 6.

Chrest, A.P., Smith, M.S., Bhuyan, S., Monahan, D.R., Iqbal, M. Parking Stuctures. 3rd Ed. Boston: Kluwer Academic Publishers, 2001.

Clifton, J.R. (1993). "Predicting the service life of concrete." *ACI Materials Journal*, 90(6), 611 – 617.

Gucunski, N., Romero, F.A., Shokouhi, P., Makresias, J. (2005). "Complementary Impact Echo and Ground Penetrating Radar Evaluation of Bridge Decks on I-84 Interchange in Connecticut." *Proceedings of the Sessions of the Geo-Frontiers 2005 Congress*, GSP 133, ASCE, Austin, TX, January 24 – 26.

Guirguis, S. (1987). "A basis for determining minimum cover requirement for durability." *Concrete durability*, ACI, Detroit, 447 – 463.

Ibrahim, M., Al-Gahtani, A.S., Maslehuddin, M., Dakhil, F.H. (1999). "Use of surface treatment materials to improve concrete durability." *Journal of Materials in Civil Engineering*, ASCE, 11(1), 36 – 40.

Khunthongkeaw, J., Tangtermsirikul, S. (2005). "Model for simulating carbonation of fly ash concrete." *Journal of Materials in Civil Engineering*, ASCE, 17(5), 570 – 578.

Liang, M.T., Lin, L.H., Liang, C.H., (2002). "Service life prediction of existing reinforced concrete bridges exposed to chloride environment." *Journal of Infrastructure Systems*, ASCE, 8(3), 76 – 85.

Liang, M.T., Zhao, G.F., Chang, C.W., and Liang, C.H. (2001). "Evaluating the carbonation damage to concrete bridges using a grey forecasting model combined with a statistical method." *Journal of the Chinese Institute of Engineers*, 24(1), 85 – 94.

Lindquist, W.D., Darwin, D., Browning, J., Miller, G.G. (2006). "Effect of cracking on chloride content in concrete bridge decks." *ACI Materials Journal*, 103(6), 467 – 473.

Minoru, K., Toshiro, K., Yuichi, U., Keitetsu, R. (2001). "Evaluation of bond properties in concrete repair materials." *Journal of Materials in Civil Engineering*, ASCE, 13(2), 98 – 105.

Puatatsananon, W., Saouma, V.E. (2005). "Nonlinear coupling of carbonation and chloride diffusion in concrete." *Journal of Materials in Civil Engineering*, ASCE, 17(3), 264 – 275.

Saetta, A.V. (2005). "Deterioration of reinforced concrete structures due to chemical-physical phenomena: model-based simulation." *Journal of Materials in Civil Engineering*, ASCE, 17(3), 313 – 319.

Smith, M.S. Shared Parking. 2nd Ed. Washington, D.C.: Urban Land Institute, 2005.

Song, H.W., Kwon, S.J., Byun, K.J., Park, C.K., "Predicting carbonation in early-aged cracked concrete." *Cement and Concrete Research*, 36(2006), 979 – 989.

Sulapha, P., Wong, S.F., Wee, T.H., Swaddiwudhipong, S. (2003). "Carbonation of concrete containing mineral admixtures." *Journal of Materials in Civil Engineering*, ASCE, 15(2), 134 – 143.

Wang, C.Y., Shih, C.C., Hong, S.C., Hwang, W.C. (2004). "Rehabilitation of cracked and corroded reinforced concrete beams with fiber-reinforced plastic patches." *Journal of Composites for Construction*, ASCE, 8(3), 219 – 228.

Weyers, R.E. (1998). "Service life model for concrete structures in chloride-laden environments." *ACI Materials Journal*, 95(5), 546 – 557.

Zhang, T., Gjorv, O.E. (2005). "Effect of chloride source concentration on chloride diffusivity in concrete." *ACI Materials Journal*, 102(5), 295 – 298.

APPENDIX A

To obtain an accurate estimate of the increased carbon dioxide concentration in a concrete parking structure, the daily traffic volume must be estimated. This data may be obtained directly from a traffic count of the structure or from the procedure described below.

ESTIMATING DAILY TRAFFIC VOLUME

1. Find "collection zone" for the parking structure

According to Smith (2005), the average driver will park within 1,600 feet of their destination. By creating a "collection zone" 1,600 feet from the perimeter of the parking structure, the destinations for drivers parking in a given structure can be identified from aerial maps.

2. Identify building types and sizes within the collection zone

Building type and size heavily influence the number of parking spaces needed for a building.

3. Calculate number of parking spaces required by each building

Table A1 estimates the number of parking spaces required base on the type and size of each building within the collection zone (Chrest et al. 2001).

Residential	
Single Family Dwelling Unit	2/Dwelling Unit
Multi-Family Dwelling Unit	
Studio	1.25/Dwelling Unit
1 bedroom	1.5/Dwelling Unit
2+ bedrooms	2/Dwelling Unit
Accessory Dwelling Unit	1/Dwelling Unit
Sleeping Rooms	1/Unit or Room
Elderly Housing	0.5/Dwelling Unit
Group and Nursing Homes	0.33/Resident
Day Care Center	1/Employee
Commercial Lodging	
Sleeping Room	1.25/Unit
Lounge	10/1,000 Sq. Ft.
Meeting Room	20/1,000 Sq. Ft.
Ballroom	30/1,000 Sq. Ft.
Hospital	
Employee	0.4/Person
Beds	0.33/Bed
Medical Staff	0.25/Person
Retail	
General	3.3/1,00 Sq. Ft.
Convenience	4/1,000 Sq. Ft.
Service	2.4/1,000 Sq. Ft.
Hard Goods	
Sales Space	2.5/1,000 Sq. Ft.
Interior/Exterior Storage	1.5/1,000 Sq. Ft.
Food and Beverage	
Fine Dining	20/1,000 Sq. Ft.
Eating and Drinking	25/1,000 Sq. Ft.
Family Restaurant	12/1,000 Sq. Ft.
Fast Food	
Kitchen	10/1,000 Sq. Ft.
Seating	0.5/Seat
Shopping Center	
Less than 400,000 Sq. Ft.	4/1,000 Sq. Ft.
More than 600,000 Sq. Ft.	4.5/1,000 Sq. Ft.

Office and Business Services	
General Business	3.6/1,000 Sq. Ft.
Consumer Service	4/1,000 Sq. Ft.
Data Processing/Telemarketing	7/1,000 Sq. Ft.
Medical Offices	6/1,000 Sq. Ft.
Industrial	
All	2/1,000 Sq. Ft.
Storage/Wholesale Utility	
All	0.5/1,000 Sq. Ft.
Educational	
Elementary and Secondary	
Classroom	1.2/Room
Driving Students	0.25/Student
College and University	To be determined
Cultural/Recreational/Entertainment	
Convention Center	20/1,000 Sq. Ft.
Public Assembly	0.25/Person
Cinemas	
Single Screen	0.5/Seat
Up to 5 Screens	0.33/Seat
Over 5 Screens	0.25/Seat
Theatres	0.5/Seat
Arenas and Stadiums	0.33/Seat
Recreation Facilities	0.33/Seat

Table A1: Summary of Space Requirements (Chrest et al. 2001)